

https://doi.org/10.1070/QEL16255

Photoresponse mechanisms of a graphene-based quantum-dot monolayer structure

Ammar J.K. Al-Alwani, A.S. Chumakov, M.V. Pozharov, E.G. Glukhovskoy

Abstract. **Hybrid structures of graphene sheets based quantum dots (QDs) are produced via Langmuir–Blodgett (LB) technique. Morphology of the structures produced is investigated by atomic force microscopy (AFM) and scanning electron microscopy (SEM). Two types of hybrid structures are prepared from graphene covered by sublayers of CdSe/CdS/ZnS and CdSe/ZnS QDs. Photocurrent properties are studied by current–voltage characteristics (CVCs) in the dark and while exposed to visible light and ultraviolet (UV) light with an excitation wavelength of 365 nm. The rise and decay times of graphene and QDs after UV illumination are estimated.**

Keywords: *photoresponse, monolayers of graphene-based quantum dots.*

1. Introduction

Graphene-based quantum dots (QDs) are very promising materials for optoelectronics applications due to high mobility of charge carriers in graphene [1]. Graphene is a very interesting material due to its high conductivity, transparency, chemical and thermal stability [2]; however, graphene sheets have a low photoresponse. Many studies are focused to overcome this obstacle by using thermoelectric effects [3] and graphene plasmons [4]. Nanocomposite-based graphene and semiconductor QDs can enhance the photoresponse of graphene. QDs as an active layer are a good harvesting material that lead to photoinduced carriers generation in QDs and their further transfer to graphene. Physical and optical properties of QDs can be changed by various factors such as size, shape and nanocomposition [5]. QDs are capped with hydrophobic organic ligands and are insoluble in polar solvents such as water.

Photogeneration of electron–hole pairs depends on the intensity of incident photons and the absorption coefficient. Graphene has a zero band gap and a graphene monolayer absorbs 2.3 % of the incident light [6]. Low photosensitivity (approximately to 10^{-3} A W^{-1}) of semi-metallic graphene [7] can be improved by covering graphene sheets with a submonolayer or multilayers of semiconductor QDs, which will make it possible to enhance light absorption by graphene [8].

Development of layered graphene sheets and semiconductor QDs for enhancing the efficiency of solar cells and photovoltic devices has been reported in work [9]. Separation of photogenerated electron–hole pairs is one of the main challenges of development of high-performance QD-based solar cells [10]. Photon absorption in semiconductor materials creates electron–hole pairs that are further separated at the heterojunction interface between QDs and graphene sheets [11].

In this work, we study monolayers of QDs and graphene at the air–water interface by the Langmuir–Blodgett (LB) technique. Two types of QDs are examined: CdSe/ZnS and CdSe/CdS/ZnS QDs. The monolayers are deposited onto a silicon substrate via the LB method. The obtained structures can be used for various applications including photodetectors and solar cells. The mechanism of photoresponse of samples is studied using current–voltage caracteristic (CVC) under various conditions.

2. Materials and methods

CdSe/CdS/ZnS and CdSe/ZnS QD solutions with concentrations of 5×10^{-6} and 10^{-5} M, respectively, have been prepared by the same method as reported previously [12]. Graphene sheets were purchased from Time-Nano Company (China), their thickness ranging from 1 to 3 nm and size varying from 2 to 10 μm. Graphene powder (3.5×10^{-4} g) was dissolved in 10 mL of chloroform and was sonicated for 20 min. The monolayers were formed at the air–water interface with water subphase having a resistance of approximately 18.2 MΩ cm at 24 °C and pH 7.0. Graphene solution (600 μL) was dropped onto the water subphase and allowed to stay there for 8 min (until chloroform evaporated completely). After that, barriers started compressing graphene sheets and formed a monolayer with a limited area. The same experiments have been performed for 50 μL of CdSe/CdS/ZnS QDs solution and 50 μL of CdSe/ZnS QDs solution. The graphene monolayer and QDs were deposited onto a silicon substrate by the vertical dipping LB technique using a KSV Nima LB Trough Medium KN 2002 setup. Thin films of QDs and graphene monolayers were investigated using scaqnning electron microscopy (SEM) and atomic force microscopy (AFM) (Nano-educator-II, NT-MDT). Their optoelectronic properties were studied by the CVC with an Agilent B1500A semiconductor device analyser and a PM5 Cascade Microtech probe station at room temperature in the dark and under illumination by a white light source (MLC-150C, Motic, Xiamen, China) and UV lamp (excitation wavelength of 365 nm; power of

Ammar J.K. Al-Alwani Saratov State University, ul. Astrakhanskaya 83, 410012 Saratov, Russia; Babylon University, Babylon, Iraq; e-mail: Ammarhamlet2013@yahoo.com;
A.S. Chumakov, E.G. Glukhovskoy Saratov State University, ul. Astrakhanskaya 83, 410012 Saratov, Russia;
M.V. Pozharov Institute of Chemistry, Saratov State University, ul. Astrakhanskay 83, 410012 Saratov, Russia

Received 16 November 2016; revision received 18 August 2017
Kvantovaya Elektronika **47** (10) 977–980 (2017)
Translated by Ammar J.K. Al-Alwani

0.5 mW cm^{-2}). The time-resolved photoresponse of the hybrid structure was investigated by recording current vs. time with periodic UV illumination at a constant voltage of 5 V applied on the structure.

3. Results and discussion

Hybrid structures of monolayers of graphene and QDs formed at the air–water intreface and deposited onto a silicon substrate using the LB technique are shown in Fig. 1.

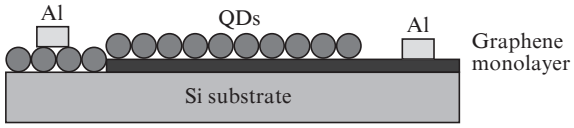

Figure 1. Graphene–quantum dot hybrid structure.

Figure 2a shows the SEM image of graphene sheets deposited onto the silicon substrate, and Figs 2b and 2c show AFM images of the surface morphology of CdSe/CdS/ZnS and CdSe/ZnS QDs, respectively. The AFM image of CdSe/ZnS QDs shows a very rough surface within the submicrometer range, while CdSe/CdS/ZnS QDs have a flat surface and good dispersion parameters. The Raman spectrum of graphene sheets exhibits two peaks at 0.1330 and 0.1586 μm^{-1}, respectively (Fig. 2d). The CVC curves for the graphene–QD hybrid structures deposited onto the silicon substrate and studied in the dark and after illumination by white light and a UV source are presented on Figs 3a and 3b. The applied voltage deviation did not exceed 0.5 V. Figure 3b depicts the CVC curves of a graphene–CdSe/CdS/ZnS QD hybrid film with a thickness varying from 20 to 25 nm. One can clearly observe asymmetric and nonlinear curves of current at various conditions with increasing current together with applied bias voltage.

The CVC curves of the graphene–CdSe/ZnS QD structure in Fig. 3a are shown as asymmetric curves because the depletion region of the interface between graphene sheets and QDs cannot be fully involved [13]. The current in the dark is 6.4×10^{-10} A (applied voltage of 0.5 V) and slighly increases under illumination by white light (6.7×10^{-10} A) and a UV source (8.0×10^{-10} A). Moreover, it should be noted that illumination also leads to a short increase in photocurrent in the region of negative voltages. The small negative photoresponse from the graphene–CdSe/ZnS QD structure can be atrributed to the surface effect of oxygen. Negligible changes of current going through this structure after illumination indicates that the internal electric field at the graphene and QD semiconductor interface is insufficient to separate the photogenerated electron–hole pairs, leading to their recombination within graphene [14].

The CVC curves of the graphene–CdSe/CdS/ZnS QD hybrid structure in the dark and after illumination by white light and UV sources are shown in Fig. 3b. The current going through this structure in the dark is equal to 1.6×10^{-10} A (applied voltage of 0.5 V). It slightly increased after exposure to visible light (up to 8.3×10^{-10} A); however, under UV illumination the current increased gradually to 9.5×10^{-9} A (which is similar to work [15] for n-type semiconductor behavior). Thus, photocurrent of the graphene–CdSe/CdS/ZnS QD

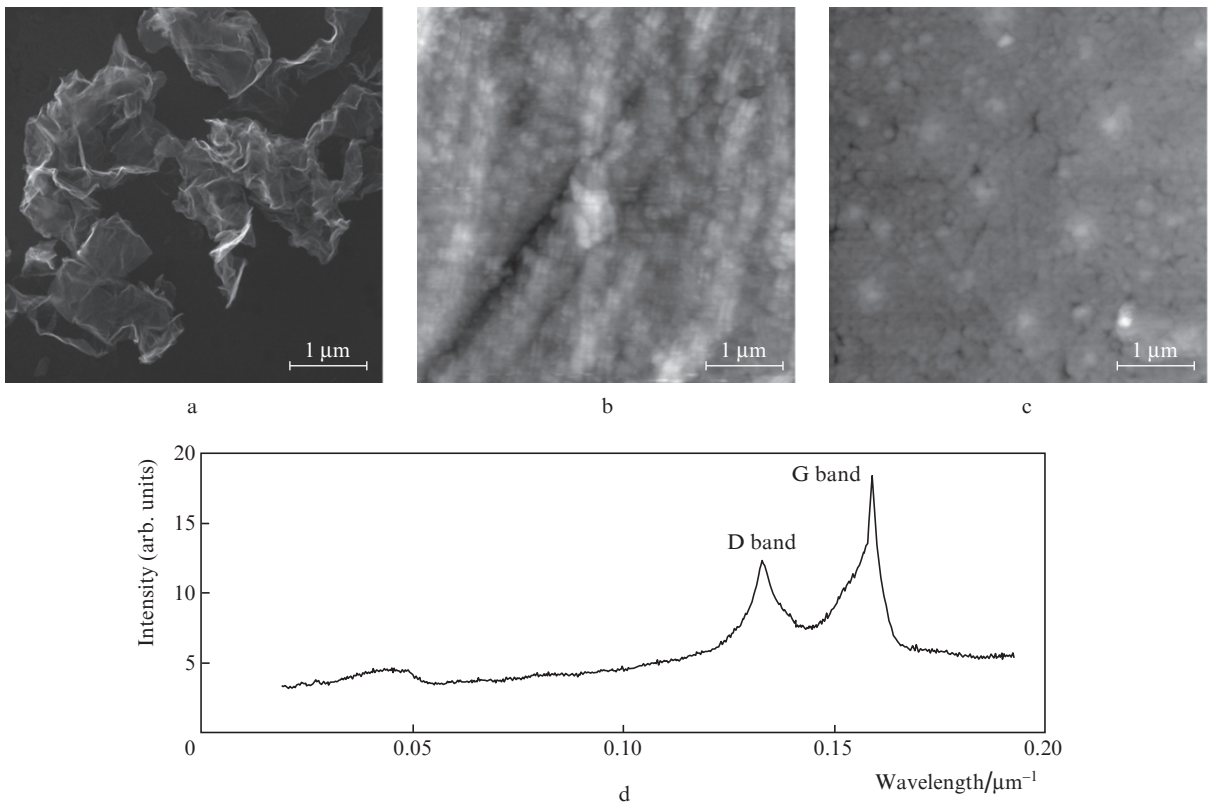

Figure 2. (a) SEM image of the graphene sheet, AFM images of (b) CdSe/ZnS and (c) CdSe/CdS/ZnS QDs, and (d) Raman spectrum of the graphene sheet.

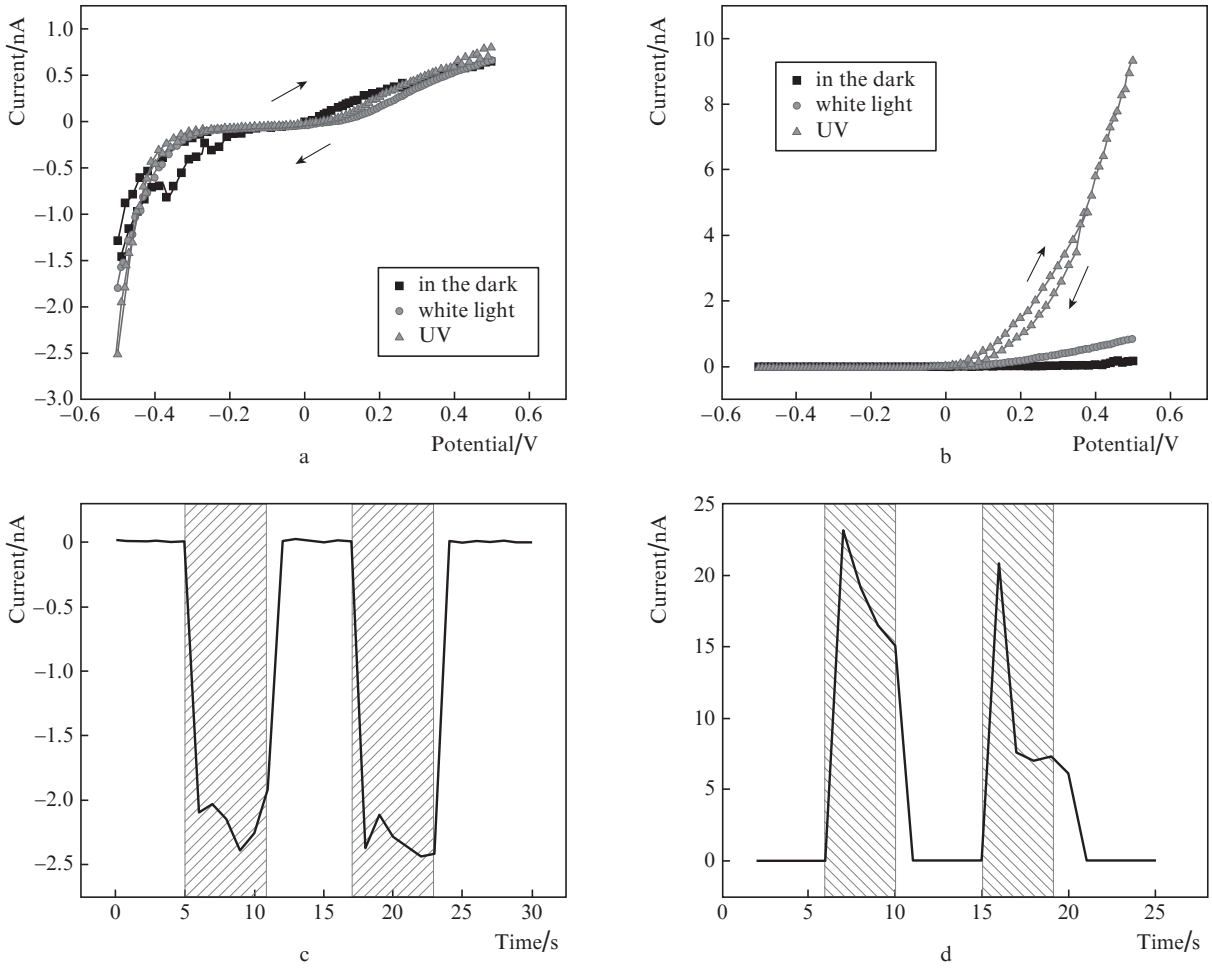

Figure 3. (a, b) CVC curves and (c, d) photoresponse of (a, c) CdSe/ZnS QD–graphene and (b, d) CdSe/CdS/ZnS QD–graphene hybrid structures. Dashed areas in Figs 3c and 3d show the regions when UV illumination is switched on.

hybrid structure is significantly higher than photocurrent of graphene CdSe/ZnS QDs under illumination by a UV source.

The changes in the CVC ratios for various described conditions are caused by absorption of the incident light and UV radiation by QDs which leads to production of additional electron–hole pairs ($h\nu \rightarrow e^- + h^+$). The electron–hole pairs generated at the surface of QDs improve current conduction, leading to an exponential growth of current [16].

The current as a function of time for the graphene–CdSe/ZnS QD hybrid structure is shown in Fig. 3c. According to the graph, a maximal photoresponse after UV illumination can be observed in the opposite direction at –0.5 V. Thus, we can assume that this structure behaves like photosensitive structures with p-type conductivity. Many authors explain this by the presence of oxygen molecules at the semiconductor surface [17, 18]. Figure 3c shows that when UV ullumination is switched on, the current changes from 9.4×10^{-13} to -2.1×10^{-9} A within a responce time of about 1 s, and when illumination is switched off, the current rapidly changes from -1.9×10^{-9} to 7.7×10^{-13} A with an approximate return time being 1 s.

Figure 3d shows the response and recovery times of the graphene–CdSe/CdS/ZnS QD hybrid structure. When UV illumination is switched on, the current increases from 1.4×10^{-11} to 2.3×10^{-8} A within 1 s; however, when UV illumination is switched off, the current decreases sharply from 1.5×10^{-8} to 1.7×10^{-11} A within less than 2 s.

Thus, a common pattern for both structures is that the absolute value of current increases with illumination and decreases when the UV source is turned off. However, in the study of the second structure, there are several noticable processes that proceed differently during illumination and have different characteristic times. When the source is switched on, there is a noticeable sharp rise in current similar to capacitor charging. This 'starting' current pulse can be associated with the generation of charge carriers and their accumulation on vacant trap states which are typically present at the interfaces [19]. Such current is limited by concentration of these trap levels, and after these levels are filled, the current disappears. According to time-dependent current patterns, there is a reason to assume that discharge of trap levels and dispersion of the localised charge proceed rather slowly. Thus, when illumination is switched on again, these levels remain partially filled and the 'starting' current pulse associated with their repeated filling is shorter and less intense.

In addition to bias current, there is also a drift current component. This part of current is more clearly visible when the light source is turned on again. The current rises to about half the level of the initialpeak which is still almost 2 orders of magnitude greater than in the dark. Using time-dependent plots we can estimate the order of magnitude of the localised charge Q by integrating the current I from time $t_1 \approx 7$ s (when the current has the maximal value) at the interval $\Delta t \approx 10$ s (after which the current ceases to vary greatly):

$$Q = \int_{t_1}^{t_1+\Delta t} I(t)\,\mathrm{d}t.$$

The charge for this structure can be approximately estimated as 5×10^{-8} C, while the state density for our geometry is approximately equal to $\sim10^{18}$ cm^{-3}. It should be noted that these parameters are estimated for the whole system (thin film and substrate) and not separate graphene or QD layers and can be used only as approximations.

As already mentioned above, interfaces can serve as places of localisation of charge carriers. The boundaries between inorganic shells of CdSe/CdS/ZnS and CdSe/ZnS QDs and boundaries between QDs and graphene sheets can act as such interfaces. It can be seen that higher complexity of the inner structure of a QD is directly correlated to a greater current flow (photocurrent values may differ by almost 2 orders of magnitude), a higher concentration of trap states leading to higher probability to capture charge carriers. Therefore, a longer lifetime of charge carriers in localised states (by several seconds) can be explained by complex relaxation mechanisms and multistage mechanisms of charge carrier migration within both quantum dots and graphene sheets [15].

4. Conclusions

Hybrid structures based on semiconductor QDs and graphene have been successfully obtained via the LB technique. AFM images of structures with CdSe/CdS/ZnS QDs show a good morphology with a lower roughness than those of CdSe/ZnS structures. It is found that exposure to UV radiation (excitation wavelength of 365 nm) leads to a singificant increase in photocurrent passing through structures of graphene sheets and QDSe/CdS/ZnS QDs. It is almost 2 orders of magnitude higher than that of graphene–CdSe/ZnS QD structures. The photoresponse of synthesised hybrid structure strongly depends on the effect of UV radiation. The characteristic relaxation times in hybrid structures consisting of graphene sheets and CdSe/CdS/ZnS QDs are equal to several seconds, which indicates the complexity of electron energy relaxation mechanisms.

Acknowledgements. The work was supported by the Russian Foundation for Basic Research (Research Project Nos 16-07-00093/16 and 16-07-00185/16).

References

1. Gromova Yu.A., Reznik I.A. *Mater. Res. Soc. Symp. Proc.*, **1787**, 15 (2015).
2. Jannik C.M., Geim A.K., Katsnelson M.I., Novoselov K.S., Booth T.J., Roth S. *Nature*, **446**, 60 (2007).
3. Echtermeyer T.J., Britnell L. *Nat. Commun.*, **2**, 458 (2011).
4. Frank H.L.K., Darrick E.C. *Nano Lett.*, **11** (8), 3370 (2011).
5. Luping X., Chenfei S., Mingbo Z., Hongling L., Nianwu L., Guangbin J., Lijia P., Jieming C. *Mater. Lett.*, **65**, 198 (2011).
6. Nair R.R., Blake P., Grigorenko A.N., Novoselov K.S., Booth T.J., Stauber T., Peres N.M.R., Geim A.K. *Science*, **320** (5881), 1308 (2008).
7. Fengnian X., Thomas M., Yu-Ming L., Alberto V.G., Phaedon A. *Nat. Nanotechnol.*, **4**, 839 (2009).
8. Chitara B., Panchakarla L.S., Krupanidhi S.B., Rao C.N. *Adv. Mater.*, **23** (45), 5419 (2011).
9. Chun X.G., Hong B.Y., Zhao M.S., Zhi S.L., Qun L.S., Chang M.L. *Angew. Chem. Int. Ed.*, **49** (17), 3014 (2010).
10. Sam-Shajing S., Niyazi S.S. *Organic Photovoltaics: Mechanisms, Materials, and Devices* (USA, FL, Boca Raton: CRC Press, 2005).
11. Konstantatos G., Badioli M., Gaudreau L., Osmond J., Bernechea M., De Arquer F.P.G., Gatti F., Koppens F.H.L. *Nat. Nanotechnol.*, **7**, 363 (2012).
12. Gorbachev I.A., Goryacheva I.Yu., Glukhovskoy E.G. *BioNanoScience*, **6** (2), 153 (2016).
13. Sachs B., Britnell L., Wehling T.O., Eckmann A., Jalil R., Belle B.D. *Appl. Phys. Lett.*, **103**, 251607 (2013).
14. Mueller T., Xia F., Freitag M., Tsang J., Avouris Ph. *Phys. Rev. B*, **79**, 245430 (2009).
15. Zhongqiang L.I., Tao D. *Proc. Biomedical Circuits and Systems Conference (BioCAS)* (USA, GE, Atlanta: IEEE, 2015).
16. Dutta M., Basak D. *Appl. Phys. Lett.*, **92**, 212112 (2008).
17. Kathalingam A., Senthilkumar V., Jin-Koo R. *J. Mater. Sci.: Mater Electron.*, **25**, 1303 (2014).
18. Kehan Y., Ganhua L., Kehung C., Shun M., Haejune K., Junhong C. *Nanoscale*, **4**, 742 (2012).
19. Nikoo S.S., Masoud L., Roohollah B., Mahdi M.B., Naimeh N., Dabirian A. *Polym. Adv. Technol.*, **27**, 358 (2016).